

Lifetime measurements of the 2^3P_1 state in heliumlike silicon and sulphur*

S. L. Varghese,[†] C. L. Cocke, and B. Curnutte

Kansas State University, Manhattan, Kansas 66506

(Received 19 July 1976)

We report measurements of the lifetime of the metastable 2^3P_1 state in heliumlike silicon and sulphur using the time-of-flight technique. An apparatus was developed suitable for direct beam-foil measurement of mean lives of x-ray emitting states whose lifetimes are in the neighborhood of 10^{-12} sec. Silicon beams at 48 and 54 MeV and sulphur beams at 50, 60, and 66 MeV underwent foil excitation in passage through a nickel foil. A high-resolution Doppler-tuned spectrometer was used to study the decay profile of the emitted x rays. The measured lifetimes of the 2^3P_1 state, $(6.35 \pm 0.33) \times 10^{-12}$ sec and $(1.57 \pm 0.18) \times 10^{-12}$ sec for silicon and sulphur, respectively, are in agreement with theory.

I. INTRODUCTION

The 2^3P_1 state in heliumlike systems decays by a fully allowed electric dipole transition to the 2^3S_1 and by a spin-forbidden electric dipole transition to the 1^1S_0 ground state. The latter intercombination transition is forbidden in the LS -coupling limit and proceeds via (relativistic) spin-orbit mixing of the 2^3P_1 state with n^1P_1 states. Because this mixing increases rapidly with nuclear charge (Z), the rate for the intercombination transition increases very fast with Z , approximately as $(Z - \xi)^{10}$ where ξ is an appropriate screening constant taken to be 0.3. Above $Z = 7$ this branch dominates the allowed decay, the latter scaling approximately as Z .

The $2^3P_1 \rightarrow 1^1S_0$ transition in light elements is a common feature in the spectrum of the solar corona¹ and of high-temperature laboratory plasmas,² and its intensity relative to that of transitions from the 2^3S_1 and 2^1P_1 states has been used³ to deduce the electron densities in such plasmas. Stimulated partially by this astrophysical interest, calculations of the rate for the transitions were made on a semiempirical basis by Elton⁴ and later by Drake and Dalgarno⁵ for the heliumlike ions up to $Z = 10$. The latter calculation showed that the $2^3P_1 - n^1P_1$ mixing, for n greater than 2, made an appreciable contribution to the rate. More recently Johnson and Lin⁶ have made a relativistic random-phase-approximation calculation of the rate for heliumlike ions through $Z = 100$.

The first experimental measurements of the lifetime of the 2^3P_1 state in heliumlike ions were made by Sellin *et al.*,⁷ in oxygen and nitrogen, using the beam-foil method. By subtracting the well-known $2^3P_1 \rightarrow 2^3S_1$ transition probability⁸ from the observed transition rates, they found the transition probability for the $2^3P_1 \rightarrow 1^1S_0$ process to be consistent with both available calculations.

Subsequent experiments by Sellin *et al.*,⁹ Mowat *et al.*,¹⁰ Moore *et al.*,¹¹ and Richard *et al.*,^{12,13} improved the mean lifetime value in oxygen and extended the measurements to fluorine. Good agreement with the calculations of Drake and Dalgarno was obtained. A summary of these results is given in Table I and Fig. 1.

Extension of the beam-foil measurements to higher Z is rendered difficult by the rapid decrease of the 2^3P_1 lifetime with Z . For silicon and sulphur the expected lifetimes are 6.3 and 1.7 psec respectively, corresponding to flight paths of 87 and 24 μm for a 1 MeV/amu beam. Since the energies for the $2^3P_1 \rightarrow 1^1S_0$ transitions in heliumlike silicon and sulphur are 1.85 and

TABLE I. Summary of results showing measured $2^3P_1 \rightarrow 1^1S_0$ transition rates for heliumlike ions.

Heliumlike system	Measured ^a rate (units of 10^{11} sec^{-1})	Theoretical rate
N	$(1.7 \pm 0.30) \times 10^{-3b}$	1.40×10^{-3i} 1.41×10^{-3j}
O	$(5.80 \pm 0.50) \times 10^{-3c}$ $(6.01 \pm 0.33) \times 10^{-3d}$ $(6.01 \pm 0.42) \times 10^{-3e}$	5.53×10^{-3i} 5.56×10^{-3j}
F	$(1.77 \pm 0.10) \times 10^{-2f}$ $(1.77 \pm 0.07) \times 10^{-2g}$	1.85×10^{-2i} 1.85×10^{-2j}
Si	1.57 ± 0.08^h	1.58^i
S	6.37 ± 0.73^h	5.87^i

^aObtained by subtracting $2^3P_1 \rightarrow 2^3S_1$ rate (Ref. 8) from directly measured total 2^3P_1 decay rate.

^bReference 7.

^cReference 9.

^dReference 12. [The error bar includes systematic effects due to background and cascade; private communication (P. Richard)].

^eReference 11.

^fReference 10.

^gReference 12.

^hPresent measurements.

ⁱReference 5.

^jReference 6.

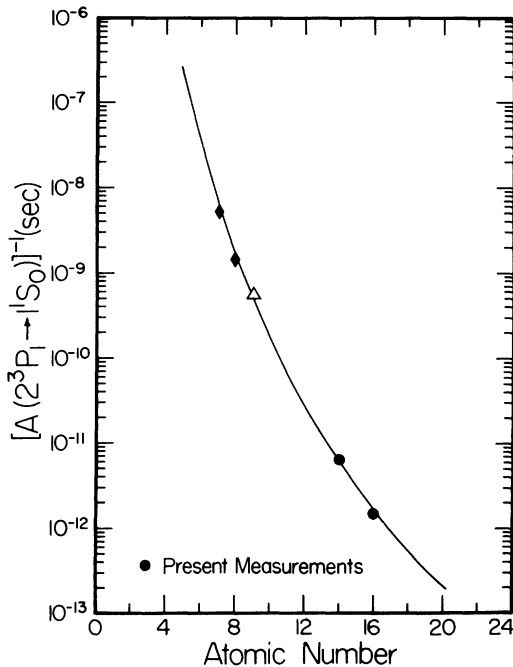


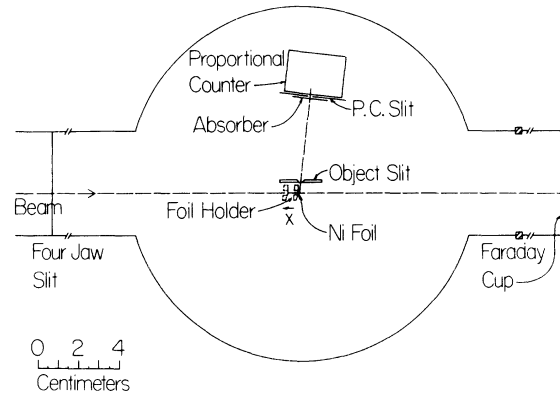
FIG. 1. Plot of the inverse of the transition rate $2^3P_1 \rightarrow 1^1S_0$ as a function of atomic number. The solid line is drawn using results from Johnson and Lin (Ref. 6). The filled circles are results from the present work. Open triangle is from the work of Richard *et al.* (Ref. 12) and Mowat *et al.* (Ref. 10) and the diamonds from Sellin *et al.* (Refs. 7 and 9). [For $Z=8$, Richard *et al.* (Ref. 13) and Moore *et al.* (Ref. 11) also have consistent numbers.] In all cases the contribution from $2^3P_1 \rightarrow 2^3S_1$ has been subtracted from the measured total 2^3P_1 decay rate.

2.45 keV respectively, a direct time-of-flight measurement requires an x-ray detector with spatial resolution of a few tens of μm . We note that resolution of this order has now been obtained with vacuum ultraviolet spectrometers and lifetime measurements in the picosecond region have been reported.^{14,15,16} To our knowledge, a comparable time resolution has not heretofore been reported in the soft x-ray region. In this paper we present direct experimental measurements of the lifetime of the 2^3P_1 states in heliumlike silicon and sulphur.

II. EXPERIMENT

A. Apparatus

The 2^3P_1 states were produced by foil exciting beams of silicon at 48 and 54 MeV and sulphur at 50, 60, and 66 MeV. The x rays from the $2^3P_1 \rightarrow 1^1S_0$ transition were tracked downstream from the exciting foil and the resulting decay profile was used to obtain the mean life of the emit-



Schematic Diagram of the Target Chamber

FIG. 2. Experimental arrangement in the target chamber shown schematically.

ting state. A schematic diagram of the apparatus is shown in Fig. 2. A high-resolution Doppler-tuned spectrometer (DTS) was used to isolate the $2^3P_1 - 1^1S_0$ line. High spatial resolution was obtained through the use of narrow object and collimating slits.

The DTS has been discussed earlier by Cocke *et al.*,¹⁷ and is similar to that described by Schmieder and Marrus.¹⁸ It utilizes a proportional counter and an absorber of a certain material and thickness with an absorption discontinuity E_{abs} . The absorber is such that near the absorption edge it will be nearly opaque to radiation with higher energy than E_{abs} and transmit very well radiation below E_{abs} . The absorber will be opaque to any radiation from the beam which is Doppler shifted so that its energy in the rest frame of the absorber is greater than E_{abs} . If E_v is the energy of the radiation in the rest frame of the ion, the critical absorption occurs at an angle θ , where θ is the angle between the line of sight of the detector and the velocity vector of the beam, such that E_v is related to E_{abs} by

$$E_v = E_{\text{abs}} \frac{1 - (v/c) \cos \theta}{[1 - (v/c)^2]^{1/2}}.$$

Here v is the ion velocity and c the speed of light. Hence, a scan of the angle θ would produce an integral spectrum with discontinuities corresponding to various spectral lines. A differential of the integral spectrum would reveal the line spectrum showing relative intensities. The advantage of the DTS is that while giving high resolution it provides higher efficiency than a crystal spectrometer of similar resolution.

A linear track moved the exciting foil in steps as small as $0.5 \mu\text{m}$. An interferometer arrangement along with a helium-neon laser was used to

check the uniformity of the track and to confirm the step size. The beams were foil excited in passage through a 5590-Å nickel foil. In addition to exciting the beams, the nickel foil was also useful in locating the downstream edge of the foil. Since the nickel $K\alpha$ line has an energy of 8.3 keV, it could be distinguished from silicon and sulphur K x rays in the proportional counter. Use of differential energy discriminators allowed simultaneous observation of nickel K x rays from the foil and K x rays from silicon or sulphur ions.

The beam was collimated to be approximately 1 mm² using the four jaw slits just outside the target chamber. The nickel foil was mounted on an aluminum holder to have the foil flat and uniform. The foil holder was attached to the linear track and a micrometer assembly through a vacuum seal. The foil could be rotated and repositioned reliably. An object slit was mounted at the center of the target chamber. It was located 5 mm from the foil and had a width of 10 μ m. A proportional counter (PC), an absorber and a PC slit (the DTS assembly) is shown. The PC slits were 100 μ m wide. The absorbers used were a 15- μ m film of SiO₂ and a 75- μ m film of polystyrene with 50% sulphur for silicon and sulphur experiments, respectively. Each data point was normalized to constant charge using the Faraday cup shown in the figure.

B. Silicon and sulphur spectra

Prior to performing the lifetime experiments we systematically studied the sulphur and silicon spectra at the foil using a DTS, similar to that shown in Fig. 2. This was done to ascertain the position of the 2^3P_1 discontinuity in the DTS spectrum. A typical DTS spectrum, smoothed as discussed in Ref. 19, from a 48-MeV silicon beam is shown in Fig. 3. In (a) of Fig. 3 the integral spectrum is shown as a function of θ . The energy scale is shown in the middle. A differential spectrum showing the heliumlike and lithiumlike lines is shown in (b). Line identification is made at the bottom of Fig. 3. The 2^3P_1 line occurs at 1854 eV corresponding to the discontinuity in the integral spectrum at 95.7°. In order to study the decay profile of the 2^3P_1 line it was necessary to take data at the top and bottom of the 2^3P_1 discontinuity. For a 48-MeV silicon beam the top and bottom of the 2^3P_1 state corresponded to 97° and 93°, respectively.

Figure 4 shows one of the DTS spectra we obtained in the sulphur experiments. As in Fig. 3, the yield vs angle or energy giving the integral spectrum is shown in Fig. 4(a). The differential spectrum is shown in Fig. 4(b). Line identifica-

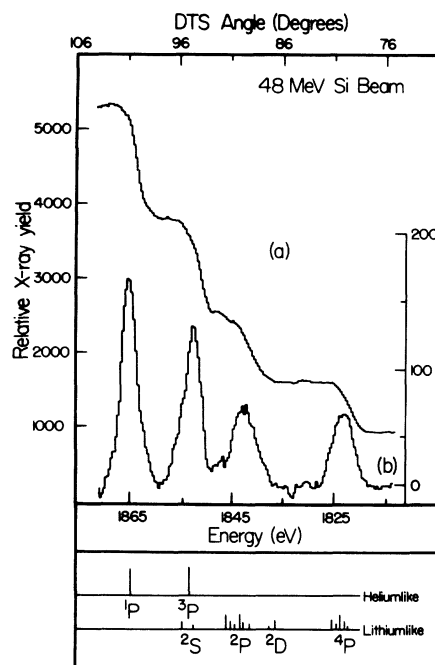


FIG. 3. (a) Integral spectrum observed using the Doppler-tuned spectrometer from a 48-MeV silicon beam. (b) Differential spectrum showing various lines. Line identification is made at the bottom part of the figure.

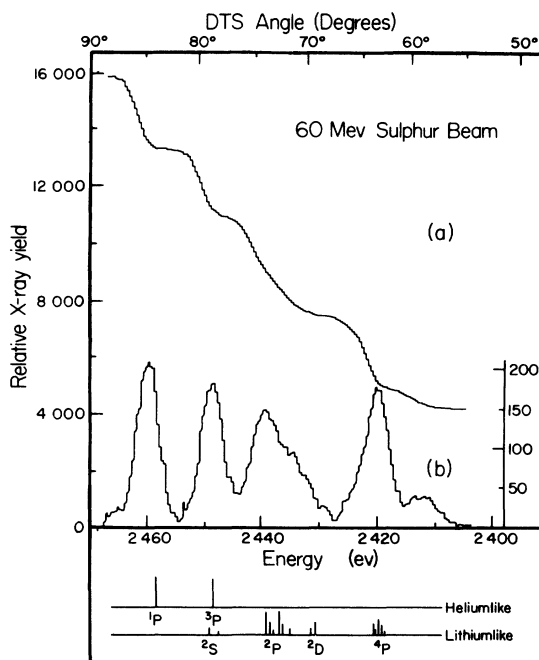


FIG. 4. (a) Integral DTS spectrum from a 60-MeV sulphur beam. (b) Line spectrum obtained by differentiating (a); heliumlike and lithiumlike contributions are also indicated.

tion is made at the bottom of the figure. The line from the 2^3P_1 state occurs at 2448 eV. The corresponding discontinuity in the integral spectrum occurred such that the top and bottom of the steps were at 82° and 78° for a 60-MeV sulphur beam. The spectral resolution obtained was about 3 eV in both the cases. It is to be pointed out that the contribution from the 2^2S and 2^2P states of the lithiumlike systems, for the case of silicon and sulphur, would not hamper the lifetime studies since both are expected²⁰ to be shorter lived by about two orders of magnitude.

C. Decay profiles

X rays from the $2^3P_1 \rightarrow 1^1S_0$ transition of sulphur and silicon as well as the nickel $K\alpha$ transition were observed using the DTS spectrometer. Simultaneous observation of nickel K x rays was important in that such an observation gave reliable alignment of the data taken on top and bottom of the 2^3P_1 discontinuity, so that subtraction would yield the correct 2^3P_1 decay profile. The Ni exciter foil was tilted such that the line of sight of the DTS remained parallel to the foil surface in all data-taking procedures.

The normalized yield of x rays, as a function of target-foil position, was taken first at the top of the 2^3P_1 step and then at the bottom. A set of curves taken using a 48-MeV Si beam is shown in Fig. 5. Separate curves for the top and bottom of the 2^3P_1 step are shown. The difference, the decay profile of the 2^3P_1 state magnified ten times, is also shown. The line drawn through the difference profile is a computer fit of the data. A discussion of the fit will be given in the next

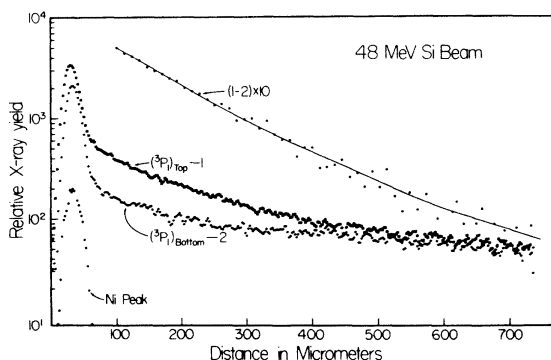


FIG. 5. Typical set of decay curves taken above and below the 2^3P_1 step in DTS spectrum of a 48-MeV silicon beam. The relative yield of x rays is plotted vs distance along the beam. The solid line through the difference, $(1-2) \times 10$, is the fit obtained to a double-exponential function. A plot of the nickel K x rays is shown to indicate the downstream edge of the foil as well as the experimental resolution.

section. The nickel K x-ray yield from the foil as a function of the foil position is also shown. The full width at half maximum of the nickel curve gives the resolution obtained. For the case of silicon experiments the measured resolution was $30 \mu\text{m}$ (FWHM). It may also be noted that the fit was begun only after the yield of Ni x rays from the foil had dropped to zero, and thus included only data well beyond the foil.

A sample set of curves obtained from a 60-MeV sulphur experiment is presented in Fig. 6. As in Fig. 5, the x-ray yields as a function of foil position for the top and bottom of the 2^3P_1 discontinuity are plotted. Also shown is the decay curve of the 2^3P_1 state of heliumlike sulphur. As before a plot of the nickel K x rays is also shown. The measured resolution from the sulphur experiments was $20 \mu\text{m}$ (FWHM). This number reflects the ultimate resolution achieved in the present experiment.

III. RESULTS AND DISCUSSION

Close examination of the decay profile of the 2^3P_1 state in both the silicon (Fig. 5) and sulphur (Fig. 6) cases shows a small contribution to the profile from a longer-lived state. We presume that the reason for this effect is perhaps a cascading process outside the foil from higher states into the 2^3P_1 state. A similar effect has been observed by Mowat *et al.*¹⁰ and Richard *et al.*¹² The apparent lifetime of this contribution was found to decrease with increasing beam energy. Because of the presence of the longer-lived component, the decay profiles were fitted to a double-exponential function of the form

$$N = N_1 \exp(-x/v\tau_1) + N_2 \exp(-x/v\tau_2) + B,$$

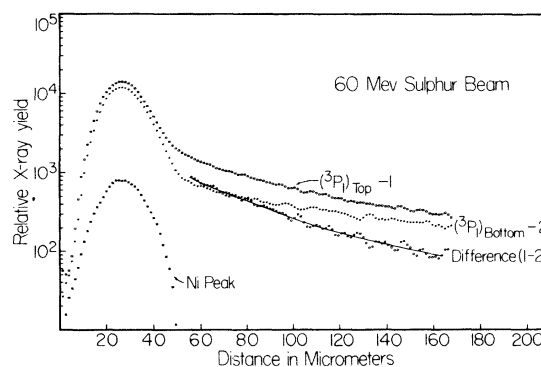


FIG. 6. Decay curves, from the 60-MeV sulphur experiment, taken on top and bottom of the 2^3P_1 step in DTS spectrum. The axes are labeled as in Fig. 5. A double-exponential fit to the difference of the two curves is the solid line. Also shown is the plot of K x rays from the foil.

TABLE II. Results of measurements made on silicon beams.

Silicon beam energy (at the foil) (MeV)		Lifetime of the 2^3P_1 state (τ_1) (10^{-12} sec)	Lifetime of the cascade (τ_2) (10^{-12} sec)	N_1/N_2
Before	After			
48	43.3	6.2 ± 0.4	16.8	16.1
54	49.6	6.7 ± 0.5	10.6	18.1
Mean-measured lifetime of the 2^3P_1 state = 6.35 ± 0.33 psec Theoretically expected lifetime = 6.33 psec ^a				

^aReference 6.

where N is the total contribution from states 1 and 2, N_1 and N_2 are the contributions from the states at $x=0$, v is the velocity of the beam, τ_1 and τ_2 the lifetimes of the 2^3P_1 state and the cascade respectively, and B , a possible background. The point $x=0$ represents the location beyond the foil at which the fit to the data began, and does not correspond to the foil position. The best fits were obtained with B equal to zero, as expected, since the decay profile is already a difference of two sets of data.

Table II gives results from the experiments on silicon beams. The first and second columns give the energy of the beam before and after the foil, respectively. The lifetime of the 2^3P_1 state of the heliumlike silicon deduced from the fitting procedure, τ_1 , is given in column 3. The fourth column gives the lifetime of the cascade, τ_2 . The last column gives the ratio N_1/N_2 . The error bar quoted with the lifetime of the 2^3P_1 state contains contributions from both statistical and systematic sources, the major part being systematic. The source of systematic error is the presence of the longer-lived weak decay. Based on the study made by Brand *et al.*²¹ on profiles containing two decays, we conservatively estimate a 5% systematic error based on the observed N_1/N_2 ratio. The weighted mean of the experimental numbers, $6.35 \pm 0.33 \times 10^{-12}$ sec, is given in the bottom of

Table II. This is in agreement with the results, 6.33×10^{-12} sec, calculated by Johnson and Lin, as shown.

Results from the sulphur experiment are shown in Table III. The quantities in Table III are categorized similarly to those in Table II. Following a similar analysis, a conservative estimate of 12% systematic error was assigned on the basis of the N_1/N_2 ratio. The weighted mean of the numbers, $1.57 \pm 0.18 \times 10^{-12}$ sec, is the measured mean lifetime of the 2^3P_1 state. As before, there is good agreement with the result of Johnson and Lin.

IV. SUMMARY

In summary we have made a moderately high-precision measurement of the lifetime of the 2^3P_1 state in heliumlike silicon and sulphur. Our results are $6.35 \pm 0.33 \times 10^{-12}$ sec for silicon and $1.57 \pm 0.18 \times 10^{-12}$ sec for sulphur. These are, to our knowledge, the first time-of-flight measurement of the lifetimes of x-ray emitting states in the picosecond region. Although these measurements reflect the present lower limit of the time-of-flight technique, we wish to point out that other measurements^{22, 23, 24} using the nonproportional yield²⁵ of x rays have extended the lower limit to include the 10^{-14} – 10^{-15} sec region.

TABLE III. Lifetimes obtained from the sulphur experiments.

Sulphur beam energy (at the foil) (MeV)		Lifetime of the 2^3P_1 state (τ_1) (10^{-12} sec)	Lifetime of the cascade (τ_2) (10^{-12} sec)	N_1/N_2
Before	After			
50	44.3	1.56 ± 0.32	7.5	2.8
60	54.3	1.57 ± 0.26	6.2	4.3
66	60.4	1.61 ± 0.43	4.0	3.9
Mean measured lifetime of the 2^3P_1 state = 1.57 ± 0.18 psec Theoretically expected lifetime = 1.70 psec ^a				

^aReference 6.

The lifetimes we have measured using the spin-forbidden transition $2^3P_1 \rightarrow 1^1S_0$ are in agreement with the recent results of Johnson and Lin, and are consistent with the results extrapolated from Drake and Dalgarno, using a $(Z - 0.3)^{10}$ scaling. Furthermore, using results extrapolated from Drake and Dalgarno for spin-orbit mixing from $2^1P_1 - 2^3P_1$ only, we conclude that by $Z = 14$ the

contribution from states higher than $n = 2$ is smaller than the precision of our experiment.

ACKNOWLEDGMENTS

We thank Russel R. Randall and Steve Spencer for assistance in data taking.

*Supported in part by ONR.

†Present address: Dept. of Physics and Astronomy, University of Oklahoma, Norman, Okla.

- ¹K. Evans and K. A. Pounds, *Astrophys. J.* **152**, 319 (1968).
²R. C. Elton and W. W. Koppendorfer, *Phys. Rev.* **160**, 194 (1967).
³A. H. Gabriel and C. Jordan, *Mon. Not. Roy. Astron. Soc.* **145**, 241 (1969); A. H. Gabriel and C. Jordan, *Phys. Lett.* **32A**, 166 (1970).
⁴R. C. Elton, *Astrophys. J.* **148**, 573 (1967).
⁵G. W. F. Drake and A. Dalgarno, *Astrophys. J.* **157**, 459 (1969); A. Dalgarno, G. W. F. Drake, and G. A. Victor, in *Atomic Physics* (Plenum, New York, 1969), p. 186.
⁶W. R. Johnson and C. D. Lin, *Phys. Rev. A* **14**, 565 (1976).
⁷I. A. Sellin, B. L. Donnally, and C. Y. Fan, *Phys. Rev. Lett.* **21**, 717 (1968).
⁸A. Weiss, in *Atomic Transition Probabilities*, NSRDS-NBS4, edited by W. L. Wiese, W. W. Smith, and B. M. Glennon (U.S. GPO, Washington, D. C., 1966), Vol. 1.
⁹I. A. Sellin, M. Brown, W. W. Smith, and B. Donnally, *Phys. Rev. A* **2**, 1189 (1970).
¹⁰J. R. Mowat, I. A. Sellin, R. S. Peterson, D. J. Pegg, M. D. Brown, and J. R. Macdonald, *Phys. Rev. A* **8**, 145 (1973).
¹¹C. F. Moore, W. J. Braithwaite, and D. L. Mathews, *Phys. Lett.* **44A**, 199 (1973).
¹²P. Richard, R. L. Kauffman, F. F. Hopkins, C. W. Woods, and K. A. Jamison, *Phys. Rev. Lett.* **30**, 888 (1973).

- ¹³P. Richard, R. L. Kauffman, F. Hopkins, C. W. Woods, and K. A. Jamison, *Phys. Rev. A* **8**, 2187 (1973).
¹⁴L. Barrette and R. Drouin, *Phys. Scr.* **10**, 213 (1974).
¹⁵D. J. G. Irwin and R. Drouin, in *Proceedings of the Fourth International Conference on Beam-Foil Spectroscopy, Gallinburg, Tenn.* (Plenum, New York, 1976), Vol. 1, p. 347.
¹⁶E. J. Knystautas and R. Drouin, in Ref. 15, Vol. 1, p. 393.
¹⁷C. L. Cocke, B. Curnutte, J. R. Macdonald, and R. Randall, *Phys. Rev. A* **9**, 57 (1974).
¹⁸R. W. Schmieder and R. Marrus, *Nucl. Instrum. Methods* **110**, 459 (1973); R. W. Schmieder, *Rev. Sci. Instrum.* **45**, 687 (1974).
¹⁹C. L. Cocke, B. Curnutte, and R. Randall, *Phys. Rev. A* **9**, 1823 (1974).
²⁰C. P. Bhalla and A. H. Gabriel, in Ref. 15, Vol. 1, p. 121.
²¹J. H. Brand, C. L. Cocke, and B. Curnutte, *Nucl. Instrum. Methods* **110**, 127 (1973).
²²H. Panke, F. Bell, H-D. Betz, W. Stehling, E. Spindler, and R. Lambert, *Phys. Lett.* **53A**, 457 (1975).
²³S. L. Varghese, C. L. Cocke, B. Curnutte, and R. Randall, *Bull. Am. Phys. Soc.* **20**, 1450 (1975); S. L. Varghese, C. L. Cocke, B. Curnutte, and G. Seaman, *J. Phys. B* (to be published).
²⁴C. L. Cocke, in Ref. 15, Vol. 1, p. 283.
²⁵H-D. Betz, F. Bell, H. Panke, G. Kalkoffen, M. Welz, and D. Evers, *Phys. Rev. Lett.* **33**, 807 (1974).